Numerical Study of Hydromagnetic Convection of an Electrically Conductive Fluid With Variable Properties Inside an Enclosure

M. Pirmohammadi, M. Ghassemi, and A. Keshtkar

***Abstract*—The buoyancy-driven magnetohydrodynamic flow in a liquid-metal-filled square enclosure is investigated by 2-D numerical simulation. The enclosure is differentially heated at two opposite vertical walls, the horizontal walls being adiabatic, and a uniform magnetic field is applied orthogonal to the gravity vector. To solve the governing nonlinear differential equations (mass, momentum, and energy), a finite-volume code based on Patankar's SIMPLER method is utilized. The results are obtained for a Rayleigh number (Ra) of 5×10^6, with a Prandtl number of 0.0091 (characteristic of Na at 150 °C) and a Hartmann number (Ha) between 100 and 700. The fluid properties are considered as a function of temperature so that the values of these properties at the hot wall are lower than that of the cold wall. It is found that the resistance to fluid motion is stronger near the hot wall and the flow intensity increases in this region. Thus, due to continuity, the form of the streamlines changes, and the symmetry of the isotherms is broken.**

***Index Terms*—Enclosure, hydromagnetic convection, variable properties.**

I. Introduction

IT IS well known that superconducting and semiconducting materials are used in electromagnetic launch technology. Some applications include superconducting ceramic rails, semiconductor armatures, electromagnetic launcher with a high-temperature superconducting magnet (HTS magnet) which launches a shuttle, superconducting electromagnetic projectile launchers, and superconducting inductive pulsed power supply for electromagnetic launchers. The Bridgman configuration is one of the important methods for the growth of semiconductor and superconductor single crystals. Investigations of heat transfer for melt flows under crystal growth conditions permit one to qualify the critical operating parameters of crystal growth. In the horizontal Bridgman technique, the molten crystal is contained in a crucible which is withdrawn horizontally from a furnace. Thus, the melt is subject to a horizontal temperature gradient, which drives the endwall convection. In practice, instabilities in the melt phase adversely affect the quality of the crystal, as they impose temperature fluctuations at the solidification front and lead to striations in the crystalline product. It is well known that unavoidable hydrodynamic movements can be damped with the help of a magnetic field. In general, the homogeneity and quality of single crystals grown from doped semiconductor melts are of interest to the manufacturers of super- and semiconductors. Hence, there has been increased interest in the flows of the liquid metals in the cavities subjected to an external magnetic field.

There exist several forces that influence natural convection. The Lorentz force is one of these forces. The influence of magnetic fields on the natural convection of various systems or processes employed for electrically conducting fluids makes an important effect on the flow and temperature distribution. Rudraiah *et al.* [1] numerically investigated the effect of a transverse magnetic field on the natural-convection flow inside a rectangular cavity with isothermal vertical walls and adiabatic horizontal walls and found out that a circulating flow is formed with a relatively weak magnetic field, that the convection is suppressed, and that the rate of convective heat transfer is decreased when the magnetic field strength increases. Al-Najem *et al.* [2] used the power law control volume approach to determine the flow and temperature fields under a transverse magnetic field in a tilted square enclosure with isothermal vertical walls and adiabatic horizontal walls at a Prandtl number of 0.71 and showed that the suppression effect of the magnetic field on the convection currents and heat transfer is more significant for low inclination angles and high Grashof numbers. Ece and Buyuk [3] illustrated the natural-convection flow under a magnetic field in an inclined rectangular enclosure heated and cooled on adjacent walls using a differential quadratic method. They demonstrated that circulation inside the enclosure, and therefore, the convection becomes stronger as the Grashof number increases while the magnetic field suppresses the convective flow and the heat transfer rate. Recently, Pirmohammadi *et al.* [4] have studied the effect of a magnetic field on the buoyancy-driven convection in a differentially heated square enclosure. They showed that the heat transfer mechanisms and the flow characteristics inside the enclosure depend strongly upon both the strength of the magnetic field and the Rayleigh number. It

Manuscript received January 11, 2010; revised June 5, 2010 and September 15, 2010; accepted September 16, 2010. Date of publication December 10, 2010; date of current version January 7, 2011.

M. Pirmohammadi is with the Islamic Azad University, Pardis Branch, Pardis New City, Tehran, Iran (e-mail: pirmohamadi@pardisiau.ac.ir).

M. Ghassemi is with the K.N. Toosi University of Technology, Tehran 19697, Iran (e-mail: ghasemi@kntu.ac.ir).

A. Keshtkar is with the Department of Engineering and Technology, Imam Khomeini International University, Ghazvin 34149-16818, Iran (e-mail: akeshtkar@ikiu.ac.ir).

Color versions of one or more of the figures in this paper are available online at http://ieeexplore.ieee.org.

Digital Object Identifier 10.1109/TPS.2010.2086081

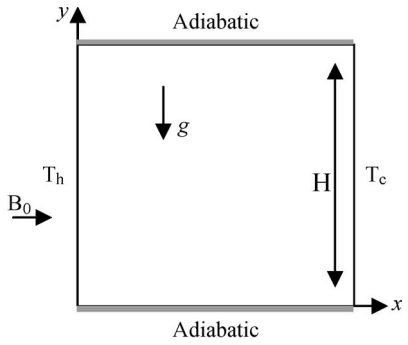

Fig. 1. Geometry and coordinates of cavity configuration with magnetic effect.

was concluded that the magnetic field considerably decreases the average Nusselt number.

In previous studies, the dependence of thermal and electrical properties on temperature has not been considered. This paper considers the laminar natural-convection flows in the presence of a longitudinal magnetic field in a square enclosure heated from the left wall and cooled from the right wall while the other walls are kept adiabatic. The enclosure is filled with an electrically conducting fluid whose thermal and electrical properties vary with temperature. The object of this paper is to obtain numerical solutions for the velocity and temperature fields inside the enclosure and to determine the effects of the magnetic field strength on the natural-convection heat transfer.

II. Mathematical Model

The steady laminar natural-convection flow in the presence of a magnetic field in a square cavity of length H was considered. The dimensional coordinates with the x-axis measuring along the bottom wall and the y-axis being normal to it along the left wall are used. The geometry and the coordinate system are schematically shown in Fig. 1.

The flow is described by the continuity, momentum, and energy equations as follows:

$$\frac{\partial u}{\partial x}+\frac{\partial v}{\partial y}=0 \tag{1}$$

$$\rho\left(u\frac{\partial u}{\partial x}+v\frac{\partial u}{\partial y}\right)=-\frac{\partial p}{\partial x}+\left(\frac{\partial}{\partial x}\left(2\mu\frac{\partial u}{\partial x}\right)+\frac{\partial}{\partial y}\left(\mu\frac{\partial u}{\partial y}+\mu\frac{\partial v}{\partial x}\right)\right) \tag{2}$$

$$\rho\left(u\frac{\partial v}{\partial x}+v\frac{\partial v}{\partial y}\right)=-\frac{\partial p}{\partial y}+\left(\frac{\partial}{\partial x}\left(\mu\frac{\partial u}{\partial y}+\mu\frac{\partial v}{\partial x}\right)+\frac{\partial}{\partial y}\left(2\mu\frac{\partial v}{\partial y}\right)\right)+\rho g\beta(T-T_r)-\sigma v B_0^2 \tag{3}$$

$$\rho\left(u\frac{\partial(c_pT)}{\partial x}+v\frac{\partial(c_pT)}{\partial y}\right)=\frac{\partial}{\partial x}\left(k\frac{\partial T}{\partial x}\right)+\frac{\partial}{\partial y}\left(k\frac{\partial T}{\partial y}\right) \tag{4}$$

where u and v denote the velocity components, p is the pressure, T is the temperature, ρ is the density, g is the gravitational acceleration, β is the coefficient of thermal expansion, and B_0 is the magnitude of the magnetic field. Moreover, k is the thermal conductivity, μ is the viscosity, c_p is the specific heat capacity, and σ is the electrical conductivity, and they vary with temperature as follows [5]:

$$\begin{aligned}
k&=91.752-48.688\times10^{-3}T-0.303\times10^{-6}T^2\\
c_P&=1437.08-580.6\times10^{-3}T+462.4\times10^{-6}T^2\\
v&=\frac{\mu}{\rho}=(0.9367-2.5806\times10^{-3}T+2.571\times10^{-6}T^2)\times10^{-6}\\
\sigma&=(13.11-33.44\times10^{-3}T+29.02\times10^{-6}T^2)\times10^{6}.
\end{aligned} \tag{5}$$

The dimensionless variables in the analysis are defined as

$$X=\frac{x}{H},Y=\frac{y}{H},U=\frac{\rho c_{pr}uH}{k_r},V=\frac{\rho c_{pr}vH}{k_r},P=\frac{\rho c_{pr}^2pH^2}{k_r^2},$$
$$\theta=\frac{T-T_c}{T_h-T_c},\sigma^*=\frac{\sigma}{\sigma_r},k^*=\frac{k}{k_r},c_p^*=\frac{c_p}{c_{p_r}},\mu^*=\frac{\mu}{\mu_r} \tag{6}$$

where σ_r, k_r, c_{pr}, and μ_r are the electrical conductivity, thermal conductivity, heat capacity, and viscosity at the reference temperature, respectively. According to the aforementioned dimensionless variables, the governing equations are given in dimensionless form as

$$\frac{\partial U}{\partial X}+\frac{\partial V}{\partial Y}=0 \tag{7}$$

$$U\frac{\partial U}{\partial X}+V\frac{\partial U}{\partial Y}=-\frac{\partial P}{\partial X}+\Pr\left(\frac{\partial}{\partial X}\left(2\mu^*\frac{\partial U}{\partial X}\right)+\frac{\partial}{\partial Y}\left(\mu^*\frac{\partial U}{\partial Y}+\mu^*\frac{\partial V}{\partial X}\right)\right) \tag{8}$$

$$U\frac{\partial U}{\partial X}+V\frac{\partial U}{\partial Y}=-\frac{\partial P}{\partial Y}+\Pr\left(\frac{\partial}{\partial X}\left(\mu^*\frac{\partial U}{\partial Y}+\mu^*\frac{\partial V}{\partial X}\right)+\frac{\partial}{\partial Y}\left(2\mu^*\frac{\partial V}{\partial Y}\right)\right)+Ra\Pr\theta-\sigma^*Ha^2\Pr V \tag{9}$$

$$U\frac{\partial\left(c_p^*\theta\right)}{\partial X}+V\frac{\partial\left(c_p^*\theta\right)}{\partial Y}=\frac{\partial}{\partial X}\left(k^*\frac{\partial\theta}{\partial X}\right)+\frac{\partial}{\partial Y}\left(k^*\frac{\partial\theta}{\partial Y}\right) \tag{10}$$

where

$$\Pr=\frac{\mu_r c_{pr}}{k_r}$$
$$Ra=\frac{\rho^2c_{pr}g\beta(T_h-T_C)H^3}{k_r\mu_r}$$

where g is the gravitational acceleration and β is the coefficient of thermal expansion. The effect of the electromagnetic field is introduced into the equations of motion (3) through the Ha number. The Hartmann number (Ha) is defined as

$$Ha=B_0H\sqrt{\frac{\sigma_r}{\mu_r}}.$$

H is the height of the enclosure.

The boundary conditions are

$$\begin{aligned} \mathrm{U\&V} &= 0 \quad \text{at all walls } (\mathrm{X}=0,\ \mathrm{X}=1,\ \mathrm{Y}=0,\ \mathrm{Y}=1) \\ \theta &= 1 \quad \text{at} \quad \mathrm{X}=0 \quad \text{and} \quad \theta = 0 \quad \text{at} \quad \mathrm{X}=1 \\ \frac{\partial \theta}{\partial \mathrm{Y}} &= 0 \quad \text{at} \quad \mathrm{Y}=0 \quad \text{and} \quad \mathrm{Y}=1. \end{aligned} \tag{11}$$

The effect of the electromagnetic field is introduced into the equations of motion through the Lorentz force term $\vec{J} \times \vec{B}$ which is the vector product of the electric current density and magnetic field inductance $\vec{B}$. The magnetic Reynolds number (Re_m) is very small in most of the engineering applications so that the magnetic field $\vec{B}$ is unchanged by the flow. The electric current density $\vec{J}$ is calculated from Ohm's phenomenological law as

$$\vec{\mathrm{J}} = \sigma(-\nabla\phi + \vec{\mathrm{V}} \times \vec{\mathrm{B}}) \tag{12}$$

where $\vec{V}$ is the velocity vector and ϕ is the electric potential. The conservation of the electric charge is

$$\nabla \bullet \vec{J} = 0. \tag{13}$$

From (7) and (8), a Poisson equation for ϕ is easily derived

$$\nabla^2 \phi = \vec{B}_0 \bullet (\nabla \times \vec{V}) = 0. \tag{14}$$

In our 2-D frame, we are left with a harmonic equation for the electric potential $\nabla^2\phi = 0$ which is valid in the melt as well as in the neighboring solid media. Since there is always, somewhere around the cavity, an electrically insulating boundary on which $\partial\phi/\partial n = 0$, the unique solution is $\nabla\phi = 0$, which means that the electric field vanishes everywhere. The Lorentz force then reduces to a systematically damping factor $-\sigma B_0^2 V$. The local Nusselt number $Nu = -\partial\theta/\partial X$ is computed at the hot wall. The average Nusselt number is expressed as $\overline{Nu} = \int_0^1 Nu_y dY$.

III. Numerical Procedures

The governing equations associated with the boundary conditions are solved numerically, employing a finite volume method. In order to couple the velocity field and the pressure in the momentum equations, the well-known SIMPLER algorithm [6] is adopted. The flow chart for the SIMPLER algorithm is shown in Fig. 2. The hybrid scheme, which is a combination of the central difference scheme and the upwind scheme, is used to discretize the convection terms. A staggered grid system [6], wherein the velocity components are stored midway between the scalar storage locations, is used. The grid dependence is investigated for the standard case. The solution of the fully coupled discretized equations is obtained iteratively using the tridiagonal-matrix-algorithm method [6]. In each iteration, the thermal and electrical properties are obtained with the calculated temperature field. Special consideration for the number of grid points is given so that the narrow Hartmann boundary layers are adequately covered at the boundaries. A fruitful discussion for the thickness of the Hartmann layers in the buoyancy-driven convection could be found in [7]. We found

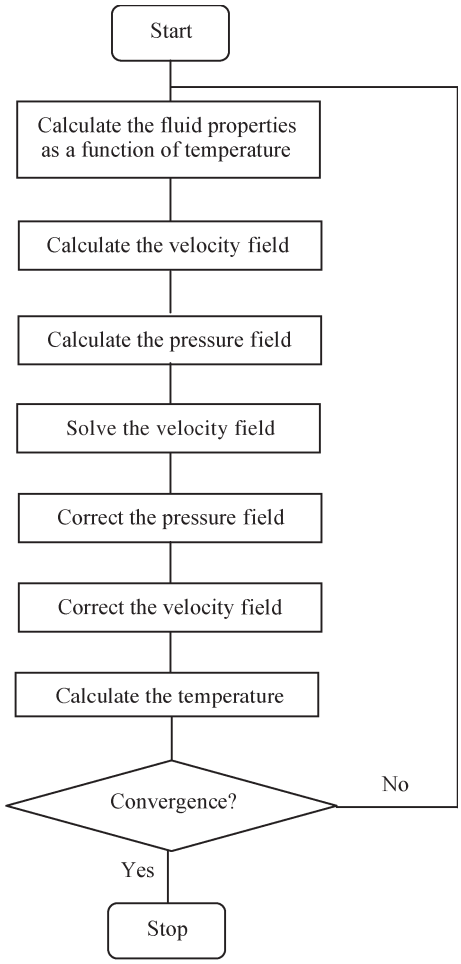

Fig. 2. Flow chart for SIMPLER algorithm.

that the 71 × 71 grid is sufficiently fine to ensure a grid-independent solution and adequately covers the thin Hartmann layers.

IV. Results and Discussion

In order to check on the accuracy of the numerical technique employed for the solution of the problem considered in this paper, it was validated by performing the simulation for the magnetoconvection flow in a square enclosure with a horizontal temperature gradient and in the presence of a magnetic field which was reported by Sarris *et al.* [8]. Fig. 3 plots the streamlines and isotherms for the present solution and the results published by Sarris *et al.* for $\mathrm{Ra} = 7 \times 10^5$, $\mathrm{Ha} = 100$, and $\mathrm{Pr} = 0.7$.

In this comparison, the properties of the fluid were assumed to be constant, and the induced magnetic field due to the motion of the electrically conducting fluid was neglected. It is observed that the results show good agreement with the Sarris work. Moreover, the relative errors of the average Nusselt number and the maximum absolute value of the stream function between the results of Sarris *et al.* [8] and the present model are 0.8% and 1.8%, respectively.

The influence of the longitudinal magnetic field (Ha) on the flow patterns and isotherms inside the enclosure for a Rayleigh

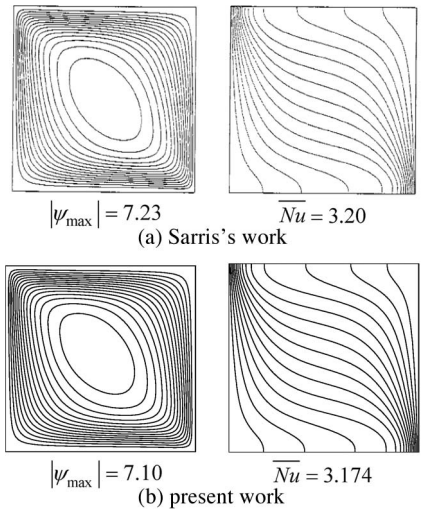

Fig. 3. (a) Isotherms and (b) streamlines of natural convection in a square enclosure for Ra $= 7 \times 10^5$ and Ha $= 100$ (the fluid properties are constant). (a) Sarris' work. (b) Present work.

number of 5×10^6 and for various Ha is shown in Fig. 4. The figures are depicted as dimensionless forms, and the streamlines and isotherms are divided into ten equally spaced intervals between the lower and higher values. As shown in (5), the fluid properties, such as μ and σ, are higher at the cold wall compared with those at the hot wall; therefore, the resistance to fluid motion is stronger near the hot wall, and the flow intensity increases in this region. Thus, due to continuity, the form of the streamlines changes. Moreover, it is seen that the isotherms are not symmetric and concentrated at the hot wall.

The flow circulation intensity, which is characterized by the maximum absolute value of the stream function, decreases as Ha increases, the stratification of the temperature field in the interior and the thermal boundary layers at the two side walls begin to diminish, and the isotherms become almost parallel to the vertical walls which indicates that the natural-convection heat transfer has been changed to the conduction mode. This is due to the retarding effect of the Lorentz force.

Fig. 5 shows the midheight velocity profiles at Ra $= 5 \times 10^6$ and for various Ha numbers. The vertical velocity V (normal to the magnetic field) interacts directly with the magnetic field and is strongly suppressed, so as shown, by increasing Ha, the peak of the velocity profile decreases. For the case of Ha $= 100$, the velocity profile is symmetric, but at higher Ha numbers, the velocity increases near the hot wall. Because the fluid properties, such as viscosity and electrical conductivity, are lower at the hot wall, therefore the Lorentz and viscous forces are lower near this wall, and the velocity is higher as well.

Fig. 6 shows the temperature profiles at Ra $= 5 \times 10^6$ and for various Ha numbers.

It is observed that, as Ha increases, the temperature profile becomes linear because, as the magnetic intensity increases, the advection suppresses and the heat transfer between the vertical walls occurs nearly by conduction.

We know from (5) that, near the hot wall, the thermal conductivity is lower than that at the cold wall, so at high Hartmann numbers at which the conduction heat transfer is dominant, the

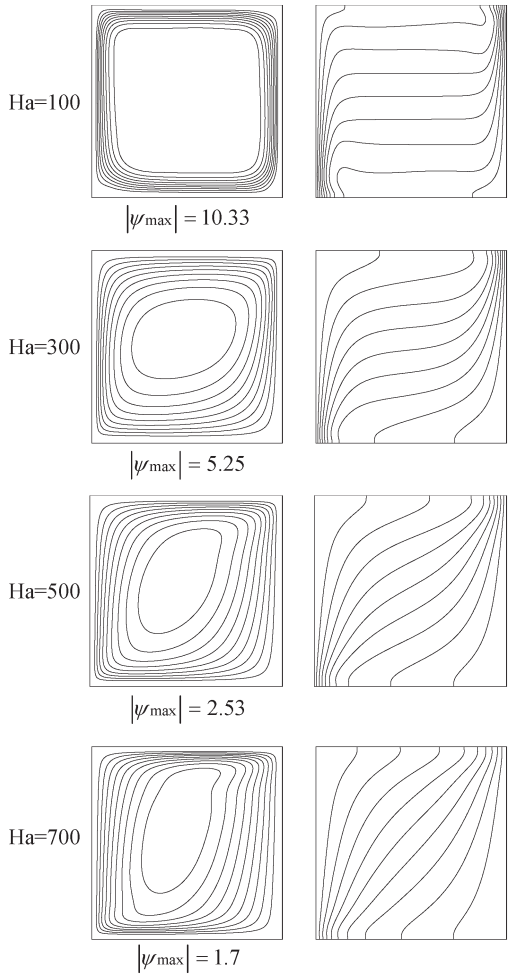

Fig. 4. (Left) Streamlines and (right) isotherms for various Ha.

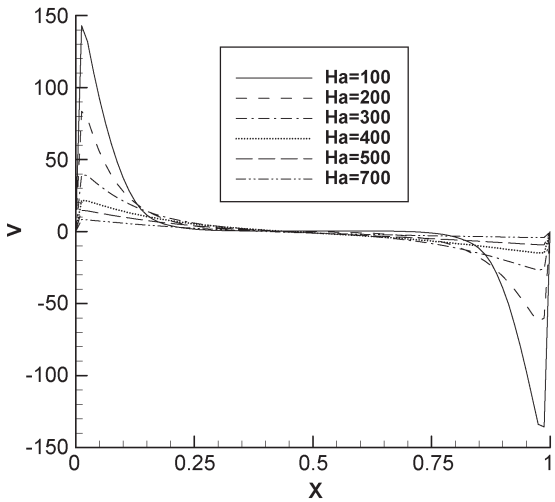

Fig. 5. Velocity profile for various Ha and at Ra $= 5 \times 10^6$.

temperature gradient and the slope of the temperature profile near the hot wall are higher than those at the cold wall.

The effects of the magnetic field on the average Nusselt number for different Hartmann numbers are shown in Fig. 7. It is evident from this figure that, with increasing Hartmann number, the Nusselt number approaches unity which indicates

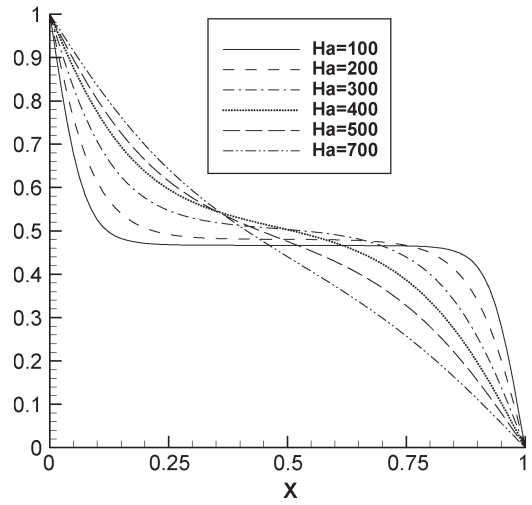

Fig. 6. Temperature profile for various Ha and at Ra $= 5 \times 10^6$.

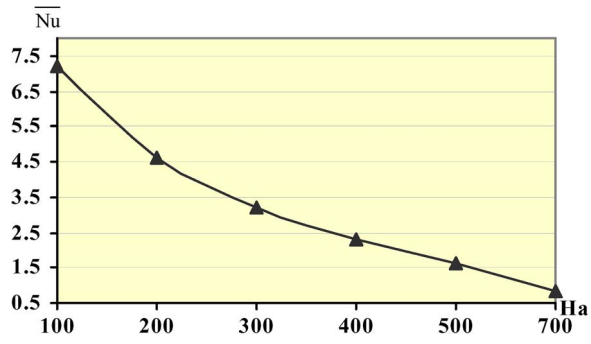

Fig. 7. Average Nusselt number in terms of Ha for Ra $= 5 \times 10^6$.

a pure conduction regime because the Lorentz force interacts with the buoyancy force and suppresses the convection.

V. Conclusion

In this paper, the magnetoconvection of the molten sodium inside a differentially heated enclosure has been numerically investigated. The thermophysical properties of fluid are considered as a function of temperature so that the values of these properties at the hot wall are lower than those at the cold wall, so because of this, the following results are found.

1) The resistance to fluid motion is stronger near the hot wall, and the flow intensity increases in this region. Thus, due to continuity, the form of the streamlines changes, and the symmetry of the isotherms is broken.
2) The Lorentz and viscous forces are lower near the hot wall because the electrical conductivity and the viscosity are lower near this wall, and therefore, the velocity increases in this region.
3) At high Hartmann numbers at which the conduction heat transfer is dominant, the temperature gradient and the slope of the temperature profile near the hot wall are higher than those at the cold wall because the thermal conductivity is lower near this wall.
4) With increasing Hartmann number, the Nusselt number approaches unity which indicates a pure conduction regime because the Lorentz force interacts with the buoyancy force and suppresses the convection.

References

[1] N. Rudraiah, R. M. Barron, M. Venkatachalappa, and C. K. Subbaraya, "Effect of a magnetic field on free convection in a rectangular cavity," *Int. J. Eng. Sci.*, vol. 33, pp. 1075–1084, 1995.
[2] N. M. Al-Najem, K. M. Khanafer, and M. M. El-Refaee, "Numerical study of laminar natural convection in tilted cavity with transverse magnetic field," *Int. J. Numer. Methods Heat Fluid Flow*, vol. 8, no. 6, pp. 651–672, 1998.
[3] M. C. Ece and E. Büyük, "Natural convection flow under a magnetic field in an inclined square enclosure differentially heated on adjacent walls," *Meccanica*, vol. 42, no. 5, pp. 435–449, Oct. 2007.
[4] M. Pirmohammadi, M. Ghassemi, and G. A. Sheikhzadeh, "Effect of magnetic field on buoyancy driven convection in differentially heated square cavity," *IEEE Trans. Magn.*, vol. 45, no. 1, pp. 407–411, Jan. 2009.
[5] U. Müller and L. Bühler, *Magnetofluiddynamics in Channels and Containers*. Wien, Austria: Springer-Verlag, 2001.
[6] S. V. Patankar, *Numerical Heat Transfer and Fluid Flow*. Washington, DC: Hemisphere, 1980.
[7] T. Alboussière, J. P. Garandet, and R. Moreau, "Buoyancy driven convection with a uniform magnetic field. Part 1. Asymptotic analysis," *J. Fluid Mech.*, pp. 545–563, 1993.
[8] I. E. Sarris, G. K. Zikos, A. P. Grecos, and N. S. Vlachos, "On the limits of validity of the low magnetic Reynolds number approximation in MHD natural-convection heat transfer," *Numer. Heat Transf.*, vol. 50, pt. B, no. 2, pp. 157–180, May 2006.

M. Pirmohammadi, photograph and biography not available at the time of publication.

M. Ghassemi, photograph and biography not available at the time of publication.

A. Keshtkar, photograph and biography not available at the time of publication.